Joint Admission and Power Control for Massive Connections via Graph Neural Network

Mengke Yang, Daosen Zhai, Ruonan Zhang, Bin Li, Lin Cai, *Fellow, IEEE*, and F. Richard Yu, *Fellow, IEEE*

***Abstract*—The sixth-generation mobile communication system (6G) puts forward higher requirement for connection density, which is difficult to meet with the existing resource management schemes in real time. In this paper, we investigate the graph neural network (GNN) based algorithms for supporting the massive connectivity in 6G. Using the power intensity of the received signal or signal-to-interference-plus-noise ratio (SINR) as a measure of communication quality, we aim to maximize the number of links that meet quality of service (QoS) requirements in a given area through joint admission and power control. Specifically, we consider two models. Among them, the blocking interference model presets the transmit power of the link in advance, and only needs admission control. After the original problem is converted to the maximum independent set (MIS) problem, we design a solution based on graph convolution network (GCN) and Q-learning. The accumulative interference model considers all the interference in the scene and controls the power and access jointly. For this model, we propose an algorithm based on graph attention network (GAT). Simulations demonstrate that the proposed GNN based algorithms preserve small computation time and achieve significant performance gain even with large network scale. As such, they are very suitable for the 6G scenario with massive connections.**

***Index Terms*—Admission control, graph attention network, graph convolution network, graph neural network, power control.**

Manuscript received 6 September 2023; revised 24 December 2023 and 23 January 2024; accepted 21 February 2024. Date of publication 28 February 2024; date of current version 15 August 2024. This work was supported in part by the National Key Research and Development Program of China under Grant 2020YFB1807003, in part by the National Natural Science Foundation of China under Grant 62271402, Grant 62232013, Grant 62171385, and Grant 62301447, in part by the Open Research Fund of National Mobile Communications Research Laboratory, Southeast University under Grant 2023D06, in part by the Key Research and Development Plan of Shaanxi Province under Grant 2023-YBGY-250, Grant 2022ZDLGY05-07, and Grant 2023-ZDLGY-06, and in part by the Natural Science Foundation of Sichuan Province under Grant 2023NSFSC1377. The review of this article was coordinated by Prof. Gabriella Olmo. *(Corresponding author: Daosen Zhai.)*

Mengke Yang, Ruonan Zhang, and Bin Li are with the School of Electronics and Information, Northwestern Polytechnical University, Xi'an 710072, China (e-mail: yangmengke@mail.nwpu.edu.cn; rzhang@nwpu.edu.cn; libin@nwpu.edu.cn).

Daosen Zhai is with the School of Electronics and Information, Northwestern Polytechnical University, Xi'an 710072, China, and also with the National Mobile Communications Research Laboratory, Southeast University, Nanjing 211189, China (e-mail: zhaidaosen@nwpu.edu.cn).

Lin Cai is with the Department of Electrical and Computer Engineering, University of Victoria, Victoria, BC V8P 5C2, Canada (e-mail: cai@ece.uvic.ca).

F. Richard Yu is with the Department of Systems and Computer Engineering, Carleton University, Ottawa, ON K1S 5B6, Canada (e-mail: richard.yu@carleton.ca).

Digital Object Identifier 10.1109/TVT.2024.3371019

I. Introduction

With the explosive growth of research on emerging communication technologies and network architectures, higher demand are put forward for data rate, latency, connectivity, coverage, and so on, which gradually exceed the capability of the fifth-generation mobile communication system (5G). Therefore, the sixth-generation mobile communication system (6G) will extend 5G to a higher level to enable various new applications, where massive Internet of Things (IoT) has great potential [1], [2], [3]. With the emerging of many innovative IoT applications such as autonomous driving, wireless brain-computer interfaces, and smart home, massive of devices will connect to the wireless networks [4]. It is predicted that the connection density, referring to the total number of communication links that can meet a specific service in a unit area, will reach $10^8/\mathrm{km}^2$ in 6G [5]. How to support this massive connectivity has become a great challenge.

As an effective mode of resource management, joint admission and power control plays a vital role in supporting the massive connectivity in wireless cellular and ad-hoc networks [6], [7], [8], [9], [10], [11], [12], [13], [14], [15], [16], [17], [18], [19], [20], [21], [22], [23], [24], [25]. In the scenario with a large number of connections, interference between links will degrade receiver signal quality, and power control only is insufficient to handle the interference. Therefore, it is necessary to optimize the system performance by joint power and admission control. In this way, admission control selects a certain number of links which can be maintained, and meanwhile power control allocates appropriate power to each transmitter. These two steps are integrated organically to alleviate the interference between links and improve the communication efficiency. For massive connectivity, the objective of joint admission and power control is to maximize the number of links that the system can accommodate from a global perspective.

To solve the joint admission and power control problem, abundant convex optimization schemes (e.g., linear programming, Perron-Frobenius theory, Lagrange duality theory, Lyapunov optimization, etc.) have been proposed over the past decades. The main drawback of the traditional schemes is of high computational complexity, which hinders their application to support massive IoT in 6G. New breakthrough technology is urgently needed, among which machine learning attracts wide attention recently [21], [22], [23], [24], [25], [26], [27], [28], [29]. The application of machine learning in resource management has

brought about the improvement of efficiency and the ability to process dynamic scenes. However, the traditional neural network has the limitation of data structure and is only applicable to European data such as image and audio, so it cannot be widely promoted in communication scenes. In contrast, graph neural network (GNN) has the ability to extract features from non-European data, which can clearly reflect the structural information of graph data. And communication systems can be naturally abstracted as graphs, so it is becoming a trend to apply GNN [30], [31] to solving the communication problems.

A. Related Work

1) Convex Optimization Based Methods: Obviously, the optimal solution of the joint admission and power control problem can be obtained by the exhaustive search algorithm, which examines every possible subset of activated links. However, the increase in the number of links will lead to a sharp rise in the computation time since the joint admission and power control problem is NP-hard [32]. The long delay is unacceptable even for a medium-scale network. Thus, plentiful suboptimal algorithms with lower computational complexity have been proposed to solve this problem.

The authors in [6] and [7] relaxed the problem as a linear programming (LP) problem, and then derived a necessary condition that is easy to check and remove the strong interfering links iteratively. Aiming at 5G networks with mixed connections of various forms, the authors in [8] designed a greedy algorithm with low complexity based on the Perron-Frobenius theory. Simulation showed that this scheme can achieve about 98% of the optimal results through exhaustive search in some cases. By using the convex optimization and Lagrange duality theory, the authors in [9] and [10] decomposed the problem into two subproblems and solved them alternately. Different from conventional scenarios, a cognitive network with primary and secondary users was considerd in [11]. Specifically, the spectral radius of the channel characteristic matrix was took as the basis to determine whether to activate the secondary link, and a hybrid admission control algorithm was designed to improve the number of activated links. Aiming at maximum spectral efficiency and network energy efficiency, the authors in [12] designed an effective algorithm for heterogeneous networks based on orthogonal frequency division multiplexing access (OFDMA) by using advanced convex approximation techniques and continuous secondary user device deflation procedures. To reduce the complexity of the algorithm, the authors in [13] derived a new relationship between a given SINR vector and its corresponding up/down power vector, based on which feasibility checks are made. Focusing on a downlink multi-input single-output system, the authors in [14] approximately converted the problem into a non-combinatorial form, and then proposed the fairness-ensuring distributed and centralized algorithms based on the Lyapunov optimization.

2) Non-Convex Optimization Based Methods: In terms of non-convex optimization, the authors in [15] proposed a method based on genetic algorithm and matching game for dealy-aware admission control and beam allocation problem in millimeter wave fronthaul downlink networks. The authors in [16] used the dynamic programming algorithm to obtain the optimal solution of the wireless network slicing and its selection problem. Considering the real-time performance of the system, the authors in [17] proposed an adaptive admission control strategy. In order to solve the admission maxization problem in multi-UAV wireless networks, the authors in [18] introduced soft admission variables and proposed an iterative algorithm. To reduce power consumption, the authors in [19] proposed a heuristic joint resource allocation and admission control strategy based on Network Function Virtualization (NFV) chains. Furthermore, to achieve the goal of maximum throughput, the authors in [20] designed a probabilistic admission control algorithm by constructing a dedicated Markov decision process.

3) Machine Learning Based Methods: Due to the limitations of the convex optimization based methods in computational complexity and performance, machine learning based methods are gradually applied to the wireless network optimization problems [21], [22], [23], [24], [25].

The authors in [21] and [22] believed that the input and output of the traditional optimization algorithms is an unknown nonlinear mapping, so deep neural network (DNN) was used to fit it. In particular, a model-free and primal-dual training mode was chosen in [22] for DNN. A large number of experiments proved that DNN has a high mapping accuracy, and more importantly, it realized a dramatic improvement in the computational efficiency. Based on the results in [21], [22], a DNN network based on geographic location data was proposed in [23] to integrate the interference information of links so as to conduct scheduling.

As a recent study, the authors in [24] put forward a new dual-criterion deep learning framework, in which geographical location information was used for network training, to achieve reasonable power allocation to users within reasonable time. In the absence of accurate channel state information (CSI), the authors in [25] designed a deep reinforcement network (DRN) for solving the joint admission and power control problem. In this scheme, the neural network was used to integrate the location distribution of users and base stations and generate an appropriate allocation scheme through iterative training.

B. Motivation

The existing algorithms have greatly improved the network performance in some aspects of indicators. Nevertheless, there are still several challenges in their application. First of all, for the convex optimization based algorithms, the problem of high time consumption is unavoidable especially in large-scale networks. When the network scenario is extended to the massive IoT, the explosive growth of connections will make the real-time control tougher. In addition, these methods are slow to respond to the environment, which means that once the environment changes, the original decision will be directly invalid and need to be re-calculated. However, the complex operation degrades the response time and it may become invalid for the highly dynamic environment. The insolvability of some problems is another important shortcoming of convex optimization based algorithms, even if the problem is approximated into a locally accessible form, there will be varying degrees of performance loss. The

non-convex optimization schemes represented by heuristic algorithm have better flexibility, but the performance varies greatly in different scenarios, and the stability is poor. The machine learning-based approach has a broader scope of application, and it does not limit the scale of the scenario and the nature of the problem. On the other hand, the performance of the machine learning based methods are easily limited by the training data. The reason is that it is difficult for the conventional neural networks to learn the relationship between links accurately, so a mass of quality data is needed for training. Moreover, there are a cumbersome number of parameters in the existing networks [21], [22], [23], [24], [25] which have great influence on the results and need to be adjusted manually. It is tedious and time-consuming to adjust these parameters.

To deal with above challenges, we consider using GNN [30], [31]. In general, graph is used to represent relationships between objects, which are matched with communication networks. Extending it to the realm of deep learning, GNN iteratively aggregates neighbors to obtain global information, thus making a more abstract representation of the graph. GNN is also suitable for unsupervised training in addition to the traditional supervised training that requires prior labels, which is implemented using the structure of graphs [33]. This training method does not rely on a large number of accurate data, which provides convenience for problem solving. In addition, different from the deep learning multi-layer complex network, GNN only needs a few simple aggregation operations (mostly 2 or 3 layers) to realize the extraction of system features, so it has the advantage of timely response.

Recently, GNN has been applied to a variety of problems in the field of communication, such as channel allocation [34], [35], power control [37], [38], [39], and topology control [36]. However, to the best of our knowledge, there is no systematic study for the GNN based link scheduling (or admission control). Consequently, in order to support the massive IoT in 6G, it is desirable to investigate the GNN based method for the joint admission and power control problem.

C. Contribution

In this paper, we study graph convolution network (GCN) [40] and graph attention network (GAT) [41] based algorithms for the joint admission and power control problem with two different models. The main contributions are summarized in what follows.

1) We consider two kinds of communication models (blocking interference model and accumulative interference model) and convert them into different types of graphs respectively. The joint admission and power control problem in the blocking interference model is formulated as a maximum independent set (MIS) problem in a directed graph. While, the problem in the accumulative interference model is formulated as a COP corresponding to a fully connected graph. The graph models will help designing the GNN based algorithms.
2) For the blocking interference model, we exploit the features of the graph and improve the existing methods of solving the MIS problem based on GCN. Specifically, in order to avoid the invalidation of nodes with high degree, we design a new degree-adaptive loss function, which changes the penalty term from a fixed value to a function that is negatively correlated with the degree of nodes. Moreover, we propose a scheme to further process the output of the network, so as to make the result more reasonable.
3) For the accumulative interference model, we put forward a GAT-based algorithm, whose network output denote the power of the transmitters. We adjust the approximation function of the step function, such that the loss function can express the solution objective more accurately. Similar to the blocking interference model, a scheme of joint admission and power control based on the network output is carefully designed to improve the number of activated links.
4) The performance of the proposed algorithms is evaluated by substantial simulations. The simulation results show that the exhaustive search method has the best performance but the maximum complexity, the heuristic algorithm has the smallest complexity but unstable performance, and the convex optimization algorithm is only suitable for small-scale scenarios. In contrast, the GNN-based algorithms proposed in this paper strike a good balance between complexity and performance, that is, they maintain small computation time and achieve significant performance gain even at large network sizes. As such, they are ideal for 6G scenarios with massive connections.

D. Notation

In this paper, variables are shown in italics, and determined quantities are shown in roman. Vectors, sets, and matrices are denoted as lowercase bold, uppercase, and uppercase bold, respectively. For a matrix $\boldsymbol{M}$, $\boldsymbol{M}^{\mathrm{T}}$ denotes its transpose form, and $\boldsymbol{M}[n]$ denotes a matrix consisting of the elements of the n-th row. $\mathbb{R}^{m\times n}$ denotes the set of $m \times n$ real matrices. Finally, $|\cdot|$ is the absolute value of a quantity. For the subscript of l, the interference link from transmitter i to receiver j is represented as ij, and the communication link from transmitter k to receiver k is represented as k.

II. Network Model and Problem Formulation

In this section, we introduce the network scenario, graph model, and problem formulation.

A. Network Scenario

As shown in Fig. 1(a) (or Fig. 2(a)), the considered network scenario is a square area with K wireless communication links indexed by $k \in \{1, \ldots, K\}$, each of which consists of a transmitter and a receiver. The channel gain from transmitter i to receiver j is denoted by h_{ij}. Let $p_k \leq \mathrm{P}_k^{\max}$ denote the transmission power of transmitter k, where $\mathrm{P}_k^{\max}$ is the power upper limit. Let $w_k \in \{0, 1\}$ denote the schedule state of link k. If link k is activated, $w_k = 1$, otherwise $w_k = 0$. Furthermore, define the power control vector by $\boldsymbol{p} = [p_1, p_2, \ldots, p_K]^{\mathrm{T}}$ and the admission control vector by $\boldsymbol{w} = [w_1, w_2, \ldots, w_K]^{\mathrm{T}}$.

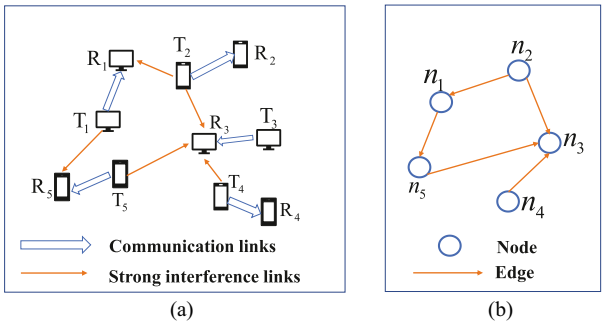

Fig. 1. Blocking interference model and corresponding graph model. (a) Communication scenario of blocking interference model. (b) Graph model converted by blocking interference model.

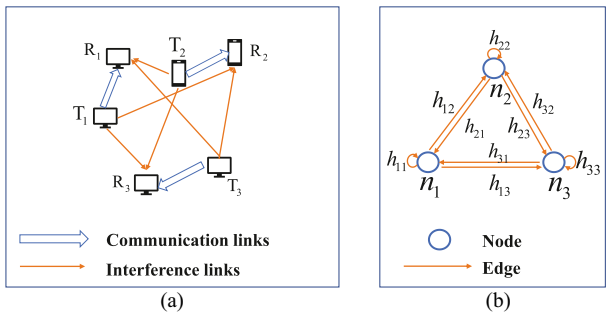

Fig. 2. Accumulative interference model and corresponding graph model. (a) Communication scenario of accumulative interference model. (b) Graph model converted by accumulative interference model.

Under such a network scenario, two typical mathematical models are developed from the point of interference, which can be generalized by blocking interference model and accumulative interference model. In what follows, we provide the detailed introduction to these two models and give the corresponding problem formulation.

B. Blocking Interference Model

When the strong interference signal power exceeds a certain value, the amplification factor of the receiver amplifier to the weak signal is reduced, or even completely suppressed, thus affecting the normal work of the system. This kind of strong interference signal is called blocking interference [42], [43]. In order to avoid this adverse phenomenon, the system design in the industrial field needs to ensure that the power of the interference signal at the input end of the receiver does not exceed the blocking level required by the system index. Based on the existence of this type of interference, we consider a joint admission and power control model named blocking interference model.

As shown in Fig. 1(a), only strong interference beyond the blocking threshold is considered in the blocking interference model. Let $N_{ij} = w_i p_i h_{ij}$ denote the interference signal power from transmitter i to receiver j. Define $\mathrm{N_t}$ as the threshold value of the strong interference signal. If $N_{ij} \geq \mathrm{N_t}$, communication link j will be interrupted. As such, we consider that device i has a blocking interference to device j if $N_{ij} \geq \mathrm{N_t}$, otherwise the effect will be ignored. The corresponding graph model is shown in Fig. 1(b). To depict this graph, we define an blocking interference link matrix $\boldsymbol{L} \in \mathbb{R}^{K\times K}$ by

$$l_{ij} = \begin{cases} 1, & \text{if } N_{ij} \geq \mathrm{N_t} \text{ and } i \neq j \\ 0, & \text{otherwise} \end{cases}. \tag{1}$$

According to the above model, blocking interference cannot be existed in the final state (If exist, the related links will be invalid). So, we only need to consider the signal-to-noise ratio (SNR). The SNR of link k can be expressed as

$$SNR_k = \frac{w_k p_k h_{kk}}{\sigma_k^2}, \tag{2}$$

where σ_k^2 denotes the noise power.

Define $\mathrm{SNR_t}$ as the minimum SNR threshold. If the condition $SNR_k \geq \mathrm{SNR_t}$ is met, the normal communication of link k is ensured. Therefore, we can set the transmission power of transmitter k as $p_k = \frac{\sigma_k^2 \mathrm{SNR_t}}{w_k h_{kk}}$, that is, the power control vector has been determined. Then, the admission control vector becomes the single factor affecting the network performance. To maximize the connections, the admission control problem can be mathematically formulated as

$$\begin{aligned} \max_{\boldsymbol{w}} \quad & card(S) \\ s.t. \quad & \textstyle\sum_{i\neq j} w_i w_j l_{ij} = 0, \\ & w_k = \{0, 1\}. \end{aligned} \tag{3}$$

where S means the set of all activated links and $card(S)$ is the number of elements in S.

C. Accumulative Interference Model

As shown in Fig. 2(a), different from the blocking interference model which only considers strong interference, entire interference in the scene are considered in the accumulative interference model. So, we should focus on the signal-to-interference-plus-noise ratio (SINR). The condition for normal communication of link k becomes $SINR_k \geq \mathrm{SINR_t}$, where $SINR_k$ denotes the SINR of link k, and $\mathrm{SINR_t}$ denotes the threshold to maintain stable communication. The expression of $SINR_k$ is given by

$$SINR_k = \frac{w_k p_k h_{kk}}{\sum_{m\neq k} w_m w_k p_m h_{mk} + \sigma_k^2}, \tag{4}$$

In this model, the interference among different devices will be serious and SINR will decrease if too many devices are activated simultaneously. We need to choose the right devices to activate and set their transmission power appropriately, to maximize the number of activated links that can meet the SINR threshold. The joint admission and power control problem in the accumulative interference model can be formulated as

$$\begin{aligned} \max_{\boldsymbol{p},\boldsymbol{w}} \quad & card(S) \\ s.t. \quad & SINR_k \geq \mathrm{SINR_t}, k \in S, \\ & 0 \leq p_k \leq \mathrm{P_k^{max}}, \\ & w_k = \{0, 1\}. \end{aligned} \tag{5}$$

Remark 1: By comparing (3) and (5), we can find that the blocking interference model only considers the strong interference as the basis for link scheduling, while the accumulative interference model considers all the interference in the scene.

Therefore, we can consider the blocking interference model as a simplified form of the accumulative interference model. By this simplification, the power control variables can be determined in advance, and the admission control problem becomes a typical MIS problem in graph theory. Therefore, we can design more efficient algorithm with lower computational complexity for the blocking interference model.

D. Convert Model Into Graph

Graphs are usually used to depict the relationships between objects. The key step in using GNN is to built the graph model. In what follow, we will go into more detail about the information contained in the graph structure.

To translate the blocking interference model into a graph, we need to obtain the node and its connection relationship but not need to more characteristics of the node or edge. As shown in Fig. 1(b), we transform it into a directed graph containing only nodes and edges. Specifically, we treat each pair of wireless communication link as a node. Furthermore, we define a matrix $\boldsymbol{L}$ to represent the blocking interference links and use it to determine the edges of the graph. An edge from node i to j will be added into the graph if $l_{ij} = 1$. Therefore, the graph converted from the blocking interference model can be expressed by $G_s = (N_s, E_s)$, where N_s represents the set of nodes, and E_s represents the set of edges. In fact, the problem in (3) is to find the MIS in $G_s = (N_s, E_s)$.

Different from the blocking interference model, the problem in the accumulative interference model requires all of the channel state to participate in optimization. Therefore, we create a weighted directed graph to represent this communication scene. As shown in Fig. 2(b), each pair of wireless communication link is abstracted as a node in the graph, which is similar to the blocking interference model. Since all devices in the scene interfere with each other, every node in the graph is connected to others. In addition, it's necessary to add a self-connected edge to each node to represent its own channel state. The initial feature of the edge from node i to j is defined as the channel gain from transmitter i to receiver j, i.e., h_{ij}. In summary, the graph converted from the accumulative interference model can be expressed by $G_p = (N_p, E_p, C_p)$, where N_p, E_p, and C_p represent the set of nodes, edges, and edge feature respectively. As can be seen, the graph in Fig. 2(b) is a fully connected graph, which is different from that in Fig. 1(b).

III. GCN Based Method for Blocking Interference Model

In this section, GCN is adopted to solve the admission control problem in the blocking interference model. We discuss the network structure of GCN, the construction of loss function for the MIS problem, and the implementation procedure of the GCN based method in the following part.

A. Network Structure

In fact, there have been some studies using GNN to solve COP. For example, aiming at the MIS problem, the authors in [44] put forward the solution scheme of Q-learning. According to the recursive neighborhood aggregation scheme, the GCN is iteratively trained on the basis of a custom loss function.

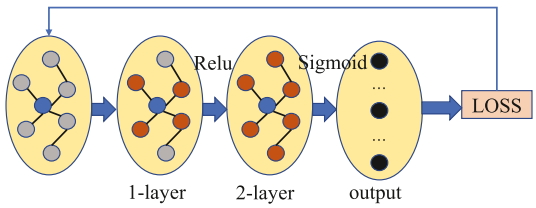

Fig. 3. Running process of GCN.

As shown in Fig. 3, each layer of GCN will aggregate the information of adjacent nodes into the current node to obtain a deeper representation. To facilitate the mathematical expression of each layer for GCN network, we denote $\boldsymbol{O}_n^d$ as the output expression of node n ($n \in N_s$) in the d-th layer. In addition, define weight matrix to be evolved during neural network training by $\boldsymbol{V}_d$ and $\boldsymbol{B}_d$. And then, the update process of GCN can be expressed as

$$\boldsymbol{O}_n^d = F_d\left(\boldsymbol{V}_d \sum_{\alpha \in \nu(n)} \frac{\boldsymbol{O}_\alpha^{d-1}}{|\nu(n)|} + \boldsymbol{B}_d \boldsymbol{O}_n^{d-1}\right), \tag{6}$$

where F means the activation function (such as $sigmoid$, $tanh$, and $relu$), $\nu(n)$ means the set of nodes which share the same edge with node n and $|\nu(n)|$ is use to standardize information about neighbor nodes.

With each additional layer of convolution calculation, the central node (or current node) can fuse the information of adjacent in a further layer. However, due to the requirements of task characteristics, nodes do not need to obtain information too far away from themselves, so the GCN network should not be too deep, usually choosing 2 or 3 layers. As shown in Fig. 3, we use 2 layers in this work.

As an important graph model, the tasks of GCN and its derived models mainly include the classification and prediction for nodes, links or graphs. In order to solve the MIS problem in the blocking interference model, we can view it as the node classification tasks. In this type of assignment, the network outputs each node's label in the form of probability. Therefore, the activation function F_2 of the second layer needs to select $sigmoid$ to modify its output into a value greater than 0 and less than 1. Furthermore, the schedule state of link k (or node k) is relaxed to O_k^2, such as

$$w_k \to O_k^2. \tag{7}$$

Moreover, define the schedule state vector by $\boldsymbol{o} = [O_1^2, O_2^2, \ldots, O_K^2]^{\mathrm{T}}$. Then, the admission control vector can be determined by

$$w_k = \begin{cases} 1, & \text{if } O_k^2 \geq 0.5 \\ 0, & \text{otherwise.} \end{cases} \tag{8}$$

Unlike F_2, F_1 can be picked flexibly. So in this case, we choose $relu$ as the activation function of the first layer.

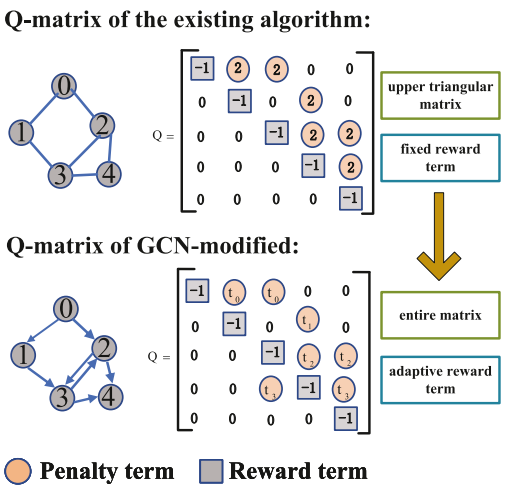

Fig. 4. Q-matrix of GCN.

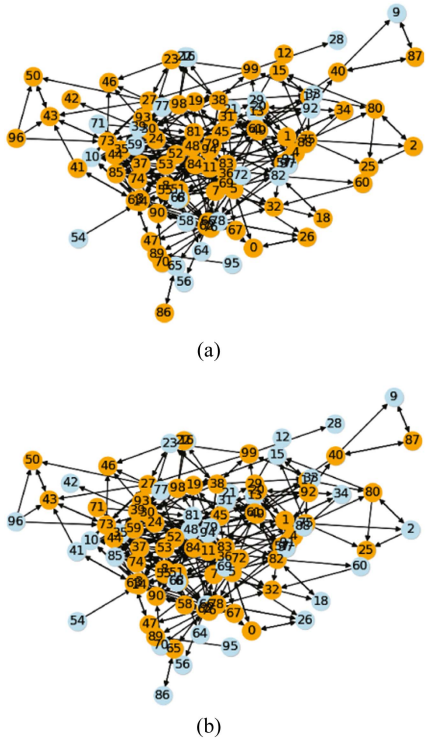

(a)

(b)

Fig. 5. Example of MIS result which the selected nodes (or the activated links) are shown in blue. (a) GCN [44]. (b) GCN modified.

B. Loss Function

The proposed algorithm refers to the pattern of using tables to construct loss functions in $\boldsymbol{Q}$-learning, so $\boldsymbol{Q}$-matrix is used for further analysis. The network updates the internal weight according to the change of the loss function, so as to output suitable results. We introduce a matrix $\boldsymbol{Q} \in \mathbb{R}^{K\times K}$ to define the loss function L_{GCN}, which is expressed by

$$L_{GCN} = \boldsymbol{o}\boldsymbol{Q}\boldsymbol{o}^{\mathrm{T}}. \tag{9}$$

As shown in Fig. 4, the loss function mainly includes two terms, i.e., reward and penalty. The reward term is set to -1, which means that when node k is selected, its contribution value to the loss function is $-{w_k}^2 = -1$. A fixed value of 2 was picked as the penalty term in [44], which will increase the loss by $2w_iw_j = 2$ if two nodes i and j with edge l_{ij} are selected at the same time. Experimental results in [44] shows that applying L_{GCN} to MIS problem can achieve excellent accuracy and efficiency.

Algorithm 1: GCN Based Method for the Blocking Interference Model.

Initialize t_k, $\mathrm{SNR_t}$, $\boldsymbol{V}$, $\boldsymbol{B}$, $\mathrm{epoch_t}$, $\mathrm{loss_t}$, lr
Each link obtains channel gains through channel estimation, determines its own transmit power, and sends the channel state and power to the host
After receiving the global information, the host generates G_s based on (1) and matrix $\boldsymbol{Q}$ based on (10)
Using graph embedding technique to generate $\boldsymbol{O}^0$
for i=1 to $\mathrm{epoch_t}$
    Layer-1:Calculate $\boldsymbol{O}^1$ by (6)
    Layer-2:Calculate $\boldsymbol{O}^2$ by (6)
    $\boldsymbol{o} = [O_1^2, O_2^2, \ldots, O_K^2]^{\mathrm{T}}$
    Calculate L_{GCN}^i by (9)
    if $L_{GCN}^i - L_{GCN}^{i-1} < \mathrm{loss_t}$
      continue
    else
      Update $\boldsymbol{V}, \boldsymbol{B}$ using the Adam optimizer
    end if
end for
Determine $\boldsymbol{W}$ by (8)
Remove conflicting nodes in order of degree of nodes from largest to smallest
Try to add links
The host sends scheduling decisions to each link

However, new problems emerge when we try to apply L_{GCN} into the blocking interference model. First of all, the form of graph is changed from undirected to directed, which makes $\boldsymbol{Q}$-matrix no longer suitably being represented by upper triangular matrix. And then, in the communication scenario of the blocking interference model, the degree distribution of nodes is not uniform, which makes it unreasonable to use a fixed penalty term. As shown in Fig. 5(a), this approach is ineffective for nodes with larger degrees. For solving the above problems, we modify the loss function as shown in Fig. 4(b). In the first step, the position of the penalty term in the $\boldsymbol{Q}$-matrix is extended from the upper triangular region to the entire matrix except the diagonal, which will be more conductive to the expression of directed graph. We add a penalty term $\boldsymbol{Q}_{ij}$ to the $\boldsymbol{Q}$-matrix when there is an edge between nodes i and j in the graph. The next step is to adjust the value of the penalty. In order to obtain a self-adaption penalty term, we adjust it from a fixed value to a function related to node degree, which makes it possible for the nodes with high degree to be selected. The penalty term appropriately decreases with the increment of node degree in the same graph, which can be expressed by

$$t_k \propto \frac{1}{de_k}, \tag{10}$$

where t_k means the penalty term and de_k means the degree of node k.

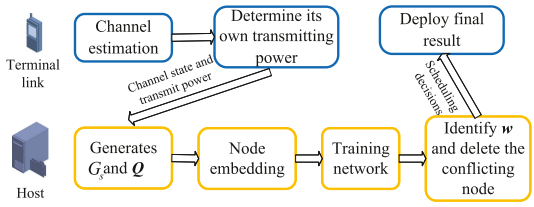

Fig. 6. Flow chat of GCN based method.

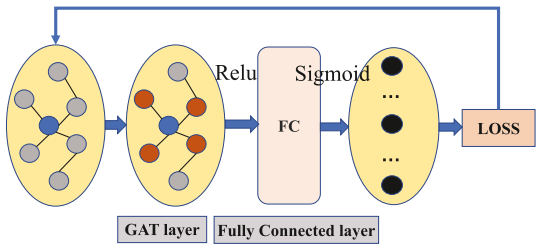

Fig. 7. Running process of GAT based method.

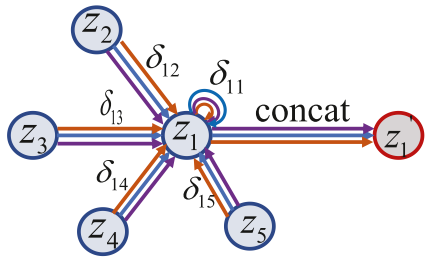

Fig. 8. 3-head graph attention mechanism.

C. Implementation Procedure

After such adjustment, the neural network will select more nodes, but the improvement of efficiency sacrifices the accuracy. So we still need to process the outputs of the neural network and screen out the final results. The detailed implementation procedure of the GCN based method for the blocking interference model is summarized in Algorithm 1, and the flow chart of the Algorithm 1 is shown in Fig. 6. An example of the result using this method is shown in Fig. 5(b). As can be seen, the result is more reasonable in comparison with that in Fig. 5(a).

IV. GAT Based Method for Accumulative Interference Model

In this section, we discuss the GAT based method for the accumulative interference model including the network structure, the construction of loss function for (5), and the implementation procedure.

A. Network Structure

GAT networks aggregate neighbor nodes through attention mechanism to realize adaptive allocation of different neighbor weights, thus greatly improving the expression ability of GNN. At the same time, we hope to obtain an adaptive admission and power control strategy according to the channel gain between different communication links in (5), which is similar to the transmission mechanism of GAT. Therefore, we consider graph attention layer as the main part of the network shown in Fig. 7.

The core of attention mechanism is to assign weight to given information. Information with high weight means that the system needs to focus on processing. To further describe this mechanism, denote **Source** as the information sources that need to be processed by the system, **Query** as some condition or a prior information, **Attention Value** as the information extracted from **Source** through the attention mechanism, and then the attention mechanism can be defined as

$$\mathbf{Attention}(\mathbf{Query}, \mathbf{Source}) = \sum_i \text{similarity}(\mathbf{Query}, \mathbf{Key}_i) \cdot \mathbf{Value}_i, \tag{11}$$

where Key-**Value** pair means each type of information,[1] similarity the correlation (the most direct way is to take inner product) between two vectors. Obviously, (11) can clearly indicate that the attention mechanism is a weighted sum of all the information **Value**, weighted by the degree of correlation between **Query** and the corresponding Key.

Multiple independent graph attention mechanisms are introduced into the GNN and the output is spliced together to form a multi-head graph attention layer. The number of heads can be selected based on the amount of data, and the magnitude of the problem is really tiny compared to the quantity scale commonly used in machine learning. So we choose the three-head graph attention layer as shown in Fig. 8, where the update of node n can be expressed by

$$\boldsymbol{Z}'_n = ||_{\xi=1}^{3} \boldsymbol{F}_\xi \left(\sum_{\alpha \in \nu(n)} \rho_{n\alpha}^{(\xi)} \boldsymbol{D}^{(\xi)} \boldsymbol{Z}_\alpha \right), \tag{12}$$

where $||$ means the concatenation operator, $\rho_{n\alpha}^{(\xi)}$ means the weight coefficient calculated by the attention mechanism of group ξ, $\boldsymbol{D}^{(\xi)}$ means the corresponding learning parameters which needs to be updated in the training process. As shown in (12) the graph attention layer has an additional dimension of adaptive edge weight coefficient compared with the update of the graph convolution layer (8), which makes the system more capable of learning.

As shown in Fig. 7, similar to GCN, each additional layer of graph attention causes the current node to acquire the characteristics of its neighbors at a further layer. Therefore, we only need to use one layer of GAT for the fully connected feature in the accumulative interference model. In order to sort out the output form of the network, we add a fully connected layer after the graph attention layer, which will enable the network to output results according to the requirements of solving objectives.

Different from the traditional scheme based on convex optimization, the key point of our proposed scheme is to treat the neural network as a power solver, which avoids designing complex problem procedures. Instead, we only need to focus

[1]We use the node embedding technology to preprocess the graph before it is introduced into the neural network, so each types of information here refer to the multidimensional node features obtained from the node embedding.

on the solution objective in the problem model, and the neural network will automatically make reasonable resource allocation for the network in the continuous learning.

To solve (5) with the neural network shown in Fig. 7, we first normalize the power of link k to

$$r_k = \frac{p_k}{\mathrm{P}_k^{\max}}. \tag{13}$$

Then, the fully connected layer requires the integration of the network output into a one-dimensional form, where the value of each element greater than 0 and less than 1 represents standardized power. Define the normalized power matrix (or network output matrix) by $\boldsymbol{r} = [r_1, r_2, \ldots, r_K]^T$. Therefore, the activation function of the fully connected layer should be determined as $sigmoid$. In addition, $relu$ is picked as the activation function for the graph attention layer in this paper which can be selected relatively arbitrarily.

B. Loss Function

The primary problem in constructing the loss function of problem (5) is to accurately represent the SINR of link k, which can be expressed as

$$SINR_k = \frac{w_k r_k \mathrm{P}_k^{\max} h_{kk}}{\sum_{m \neq k} w_m w_k r_m \mathrm{P}_m^{\max} h_{mk} + \sigma_k^2}. \tag{14}$$

First of all, we assume that all the links are activated because the neural network is used for the initial solution of power, then the expression is modified as

$$SINR_k = \frac{r_k \mathrm{P}_k^{\max} h_{kk}}{\sum_{m \neq k} r_m \mathrm{P}_m^{\max} h_{mk} + \sigma_k^2}. \tag{15}$$

We define two auxiliary matrix $\boldsymbol{Q}_1, \boldsymbol{Q}_2 \in \mathbb{R}^{K \times K}$ by

$$\boldsymbol{Q}_1 = \begin{bmatrix} \mathrm{P}_1^{\max} h_{11} & & & & \\ & \cdots & & & \\ & & \mathrm{P}_i^{\max} h_{ii} & & \\ & & & \cdots & \\ & & & & P_K^{\max} h_{KK} \end{bmatrix}, \tag{16}$$

$$\boldsymbol{Q}_2 = \begin{bmatrix} 0 & \mathrm{P}_1^{\max} h_{12} & \cdots & \cdots & \mathrm{P}_1^{\max} h_{1\,K} \\ \cdots & 0 & \cdots & \cdots & \cdots \\ \mathrm{P}_i^{\max} h_{i1} & \mathrm{P}_i^{\max} h_{i2} & 0 & \cdots & \mathrm{P}_i^{\max} h_{iK} \\ \cdots & \cdots & \cdots & 0 & \cdots \\ \mathrm{P}_K^{\max} h_{K1} & \mathrm{P}_K^{\max} h_{K2} & \cdots & \cdots & 0 \end{bmatrix}. \tag{17}$$

Furtherly, $SINR_k$ can be regarded as a function with $\boldsymbol{R}$ and rewritten as

$$SINR_k(\boldsymbol{r}) = \frac{\boldsymbol{r}^{\mathrm{T}} \boldsymbol{Q}_1[k]}{\boldsymbol{r}^{\mathrm{T}} \boldsymbol{Q}_2[k] + \sigma_k^2}. \tag{18}$$

As we all know, the loss function must meet the differentiable condition in the process of network training, no matter which method is selected for solving optimization problems (such as Newton's method, gradient descent method, maximum likelihood estimation method, etc.). However, the objective function in (5) which can be expressed by

$$card(\boldsymbol{S}) = \sum_k \delta[SINR_k(\boldsymbol{r}) - \mathrm{SINR_t}] \tag{19}$$

is a step function based on $SINR_t$. So we need to select an approximation function to transform it into a differentiable form. $Sigmoid$ is a good approximate form of the step function. We modified it by shifting it a certain distance to the left according to the requirements of the problem. We denote this modified function as Ψ, then the loss function of the neural network can be expressed as

$$L_{GAT} = -\sum_k \Psi[SINR_k(\boldsymbol{r}) - \mathrm{SINR_t}]. \tag{20}$$

This correction can effectively alleviate the network training in the direction of too large SINR of a single link, which will lead to resource waste and efficiency reduction.

Algorithm 2: GAT Based Method for the Accumulative Interference Model.

```
Initialize P^max, SINR_t, ρ, D, epoch_t, loss_t, lr
Each link obtains channel gains through channel estimation and sends them to the host
After receiving the global information, the host generates G_p based on Fig. 2 and matrix Q_1, Q_2 based on (16) and (17)
Using graph embedding technique to generate Z^0
for i=1 to epoch_t
    Layer-1:graph attention layer
    Layer-2:fully connected layer
    r = [r_1, r_2, ..., r_K]^T
    Calculate L^i_GAT by (20)
    if L^i_GAT − L^{i−1}_GAT < loss_t
      continue
    else
      Update D using the Adam optimizer
    end if
end for
The host determines p by r and sends it to each link
Each link adjusts its scheduling status by (21)
Select the link corresponding to the maximum SINR and adjust its transmit power by (22) until the system is stable
Each link measures its own SINR and determines p
```

C. Implementation Procedure

We can preliminarily get the SINR of link k (i.e., $SINR_k$) from the output values on node k (i.e., r_k) of the network by (15). Naturally, we activate the link which SINR is greater than $\mathrm{SINR_t}$. Besides, a constant $\mathrm{SINR_l}$ ($0 < \mathrm{SINR_l} < \mathrm{SINR_t}$) is introduced to initially determine the schedule state of the rest of links. The above steps can be expressed as

$$w_k = \begin{cases} 1, & \text{if } SINR_k \geq \mathrm{SINR_t} \\ 0, & \text{if } SINR_k < \mathrm{SINR_l}. \end{cases} \tag{21}$$

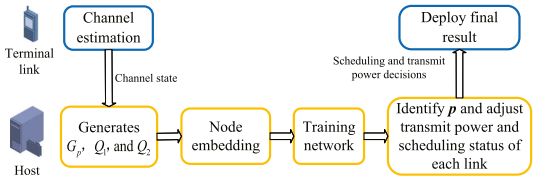

Fig. 9. Flow chat of GAT based method.

A certain number of links with SINR slightly lower or larger than $\mathrm{SINR_t}$ exist since the neural network loss approximates the objective function, which leads to a waste of resources. We set r_k to 0 for an inactivated link k (or $w_k = 0$).

To further improve the network performance, we adjust the link power that causes resource waste. It can be inferred from (14) that reducing the SINR of one link $SINR_k$ increases the SINR of all links except k. Therefore, for the link a with the largest SINR in the current scene whose SINR is η times as large as $\mathrm{SINR_t}$, we reduce r_a to $\frac{1}{\eta}$ times of the original, which can be formulated by

$$r_a \to \frac{r_a}{\eta}, \tag{22}$$

where $\eta = \frac{SINR_a}{\mathrm{SINR_t}}$. By reducing the power of these links, the method can effectively improve the performance of the links whose SINR is slightly lower than $\mathrm{SINR_t}$ to meet the decoding threshold. We continue to select a new link with the maximum SINR until all links meet the decoding threshold described in Algorithm 2. In this case, the number of activated links will be effectively improved.

Then, the operation is to determine the final admission control according to the SINR, which can be described by

$$w_k = \begin{cases} 1, & \text{if } \mathrm{SINR}_k \geq \mathrm{SINR_t} \\ 0, & \text{else,} \end{cases} \tag{23}$$

where $SINR_k$ is calculated by $\boldsymbol{r}$ modified via (15). The GAT based method for the accumulative interference model is summarized in Algorithm 2, and the flow chart of the Algorithm 1 is shown in Fig. 9.

V. Simulation Results and Performance Analysis

In this section, we conduct simulation to evaluate the performance of our proposed algorithms. The architecture of GNN is implemented by using the open-source library dgl.nn in Python 3.9.13. Besides, the environment platform used for simulation include PyChram 2022, Anaconda 3, and Torch 1.10.0. For the simulation scenario, we randomly place several pairs (from 20 to 10000) of transmitters and receivers in a square area with its side as 2 km as depicted in Fig. 1(a). The receiver of each link is randomly distributed within a circular range of 100 m from the corresponding transmitter while the distance between each transmitter is not limited. We use the free space pass loss (FSPL) as the channel model. The common scenario parameters are summarized in Table I, and only parts will be modified in different simulations.

TABLE I
Simulation Parameters

Parameter	Value
Length of square area	2 km
Range of Tx-Rx distance	100 m
Carrier frequency	2400 Mhz
Number of links, K	20-10000
Path loss model	$100 + 20lg(d)$
Noise Power, σ_k^2	10^{-10}
Blocking Interference threshold, $\mathrm{N_t}$	1
SNR threshold, $\mathrm{SNR_t}$	5 dB
SINR threshold, $\mathrm{SINR_t}$	5 dB
Dimensions of node embedding, ed	$\sqrt{K}$
Hidden layer size, hl	$\sqrt{K}/2$
Maximum number of epochs, $\mathrm{epoch_t}$	20000 (Algorithm 1)
Maximum number of epochs, $\mathrm{epoch_t}$	2000 (Algorithm 2)
Learning rate, lr	0.0001
Loss function reduction threshold,$\mathrm{loss_t}$	0.0001
Optimization algorithm	Adam
Penalty term, t_k	$4.6/de_k$
Approximation function, Ψ	$sigmoid(x + 0.4SINR_t)$
Output layer size	1

A. Performance Evaluation for the GCN Based Method

1) Simulation Settings for the GCN: We use a two-layer GCN whose hidden layer size is determined by the number of communication links in the scene (or the number of nodes in the graph). The detailed parameters of the network is described as Table I.

2) System Performance in Samll-Scale Scene: We scale down the scene, which means that the size of the square area vary with the number of communication links. The length and distance shrink by a factor of $\sqrt{s}$ if the corresponding number of communication links shrinks by a factor of s. In this scene, we compare Algorithm 1 with the exhaustive search algorithm in terms of computational complexity and the number of activated links.

In order to evaluate the computational complexity of Algorithm 1, we set the number of links ranging from 30 to 45, and the results of the running time is shown in Table II. The simulation results reveal that the running time of the exhaustive search algorithm increases sharply with the increase of links, which is due to the fact that the MIS problem is NP-hard. In sharp contrast to the exhaustive search algorithm, the operation time of Algorithm 1 is small and almost keeps the same vale with the increase of links. The main reason is that dgl.nn library adopts an efficient layer by layer propagation rule to implement GCN, which improves the computational efficiency.

In addition, we also compare the number of activated links obtained by the two algorithms to demonstrate the performance of Algorithm 1. It can be confirmed through the Table II that in the small-scale scene, the average number of activated links obtained by Algorithm 1 can reach 83.8% of the optimal value, which is acceptable compared with the traditional optimization algorithms. Therefore, when the number of links is very large (i.e., large-scale networks), Algorithm 1 can provide relatively good solutions with high computational efficiency.

To analyze system performance in middle and large scale scenes, we compare Algorithm 1 with the other two algorithms.

TABLE II
PERFORMANCE OF ALGORITHM 1 IN SMALL-SCALE SCENE

Number of links		Exhaustive search	Algorithm 1	percentage
30	Number of activated links	19.74	16.62	84.2%
	running time	34.92s	39.87s	114.2%
35	Number of activated links	21.96	18.53	84.4%
	running time	467.83s	42.36s	9.1%
40	Number of activated links	23.38	19.56	83.7%
	running time	3817.59s	44.23s	1.2%
45	Number of activated links	25.44	21.16	84.2.2%
	running time	25757.93s	46.2s	0.2%

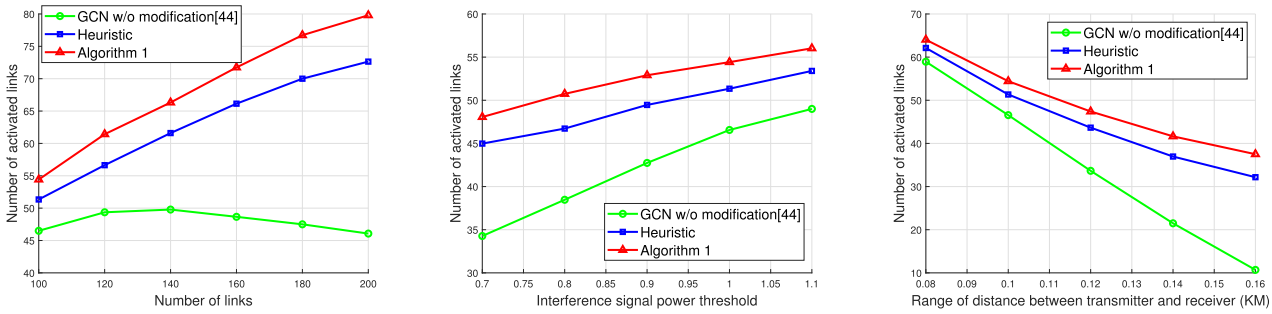

(a) (b) (c)

Fig. 10. Simulation results in middle-scale scene. (a) Number of activated links with different number of links. (b) Number of activated links with different interference signal power threshold. ($K = 100$). (c) Number of activated links with different Tx-Rx distance. ($K = 100$).

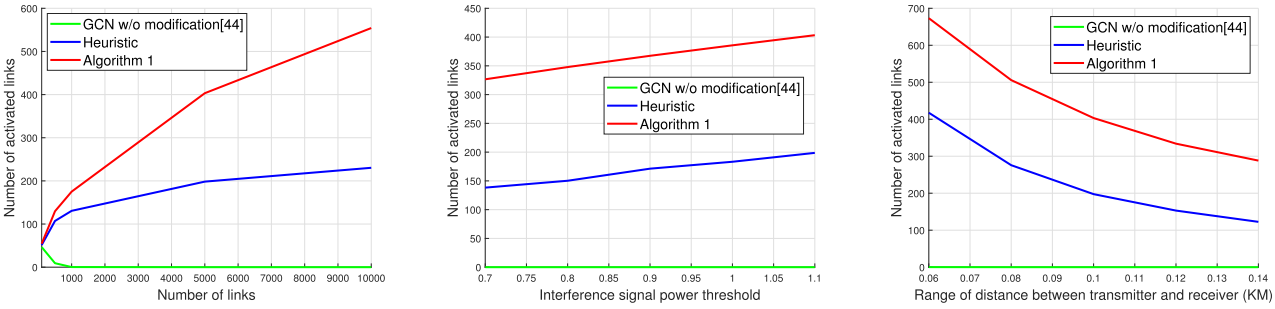

(a) (b) (c)

Fig. 11. Simulation results in large-scale scene. (a) Number of activated links with different number of links. (b) Number of activated links with different interference signal power threshold. ($K = 5000$). (c) Number of activated links with different Tx-Rx distance. ($K = 5000$).

The first one is proposed in [44], which is represented by "**GCN w/o modification**". Moreover, we choose a traditional **heuristic** algorithm for the MIS problem, which is implemented with an open source package named networkx in Python 3.9.

3) Effect of Link Number on System Performance: Figs. 10(a) and 11(a) show the number of activated links versus different number of communication links in middle and large scenes described by Table I. It can be observed that the total number of activated links by Algorithm 1 and **heuristic** algorithm grow steadily as the number of links increases. Nevertheless, the curve of **GCN w/o modification** shows a downward trend. The main reason is that the node degree in graph raises with the link number, and the fixed penalty term in the Q-matrix is invalid for nodes with large degree. When the number of links increases to 1000, **GCN w/o modification** fails completely. Unlike this method, the adaptive penalty factor used in Algorithm 1 combats the effect of node degree.

4) Effect of Blocking Interference Signal Power Threshold on System Performance: We change the scenario with N_t from 0.7 to 1.1 in order to investigate the effect of different interference signal power threshold on system performance, which is shown in Figs. 10(b) and 11(b). Obviously, the interference radius of the transmitter is inversely correlated with this parameter, which leads to fewer edges between nodes and hence more independent nodes. The rising lines in Fig. 10(b) clearly demonstrate this conclusion. Furthermore, Algorithm 1 still greatly outperforms the other two algorithms under different N_t. The nodes degrees in large-scale scene exceed the application range of **GCN w/o modification**, which makes the corresponding number of activated links in Fig. 11(b) and (c) 0.

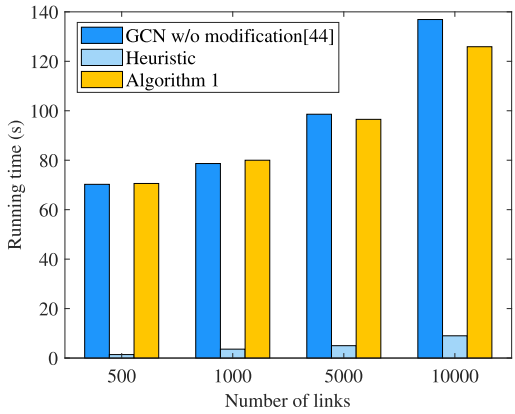

Fig. 12. Running time of blocking interference model.

5) Effect of Tx-Rx Distance on System Performance: Figs. 10(c) and 11(c) illustrate how the range of the distance between transmitter and receiver affects the total activated links. When the distance is short, the performance of the three algorithms is very close. However, with the increase of the distance, **GCN w/o modification** decreases sharply compared with others. The reason is that the receiver is far away from the transmitter and the transmission power increases, thus the blocking interference range of the transmitter expands naturally. This phenomenon corresponds to the increase in node degree, which makes the performance loss of **GCN w/o modification**. By contrast, this negative effect is weakened in Algorithm 1 through the dynamic adjustment of the loss function.

6) Computation Complexity: Fig. 12 shows the running time of several algorithms at different scene scales. The heuristic algorithm can find the independent set by obtaining the local optimal solution. It only needs to compare the degree of the existing nodes, and can run with high efficiency. The running time of **GCN w/o modification** and Algorithm 1 is mainly occupied by the training network. When **GCN w/o modification** does not fail ($K \leq 1000$), the running time of Algorithm 1 will be slightly longer, which is the time used for subsequent checks and adjustments. Otherwise, the network is difficult to converge after the number of nodes increases for **GCN w/o modification**, so the running time will be longer.

Remark 2: Each operation in this work only sends one instance to network for training, that is, it does not distinguish the training and testing process, and the running time refers to the whole process from sending a scene into the computer to making a decision.

B. Performance Evaluation for the GAT Based Method

1) Simulation Settings for the GAT: The simulation settings in this part are similar to that in Section V-A, and the network parameters for the GAT are listed in Table I.

2) Consistency of Loss Function and Solution Objective: To verify the validity of our constructed loss function, we take the opposite number to the loss and compare it with the number of activated links determined from the network output. Fig. 13 reveals an example that the change trend of the activated link number is consistent with the loss. At the same time, the convergence rate of the network is very fast. After 800 iteration epochs, the loss and solution objective tend to be stable, which proves that the method we proposed is efficient.

In addition, in order to verify the influence of different parameters on network performance, we select three network parameters (learning rate, hidden layer size and dimensions of node embedding) for adjustment. Fig. 13 shows that the efficiency and performance of the system are slightly different due to the change in parameters, but convergence and relatively impressive results can still be guaranteed, which proves that the excellent effect of our proposed scheme is not obtained through the coincidence of parameter adjustment, but the function of the network model itself. Specifically, the higher the learning rate, the faster the convergence speed. The hidden layer size and the dimensions of node embedding increase the number of trainable weights, thereby trading network complexity for superior performance, which can be revealed in Fig. 13(b) and 13(c). The network parameters selected by weighing computational load and network performance are shown in Table I.

In the following part, we compare Algorithm 2 with the other two algorithms. Linear programming is a traditional way to solve the joint admission and power control problem, and the scheme proposed in [6] is a typical representative which is denoted by LP in the subsequent discussion. Moreover, GAT in [41] can be directly used for solving the problem in (5), and we denote it as **GAT w/o modification**. Different from Algorithm 2, the operations in Section IV-C are not implemented for the output of **GAT w/o modification**.

3) Effect of Link Number on System Performance: In order to study the impact of link number on system performance, we set the number of links between 20 and 10000. Figs. 14(a) and 15(a) clearly demonstrate that the performance of all algorithms can be improved steadily with the increase of links in the scenario. We can find that the number of activated links in Fig. 14(a) is smaller than that in Fig. 10(a) under the same parameters settings. This is due to the accumulative interference is considered, which makes it difficult for the system to allocate the right transmission power to each link. In brief, Algorithm 2 achieves an average performance improvement of 43.78% over LP and 10.37% over **GAT w/o modification** across all the simulation environments.

Noted that the GAT-based algorithm also has the advantage in computational complexity. Fig. 15(a) shows that in large-scale scenes, when the number of links increases to more than 2000, the time required for **LP**-based algorithm becomes unbearable and Algorithm 2 can still maintain efficient resource allocation. Therefore, in the subsequent simulation to large-scale scenes, in order to enable the comparison of different algorithms, 2000 is selected as the standard number of links, which are shown in Fig. 15(b) and 15(c).

4) Effect of SINR Threshold on System Performance: Figs. 14(b) and 15(b) show the system performance when $SINR_t$ changes from 4 to 9 dB. Obviously, the increase of SINR threshold makes more links unable to meet the communication requirement, and Algorithm 2 is more sensitive to

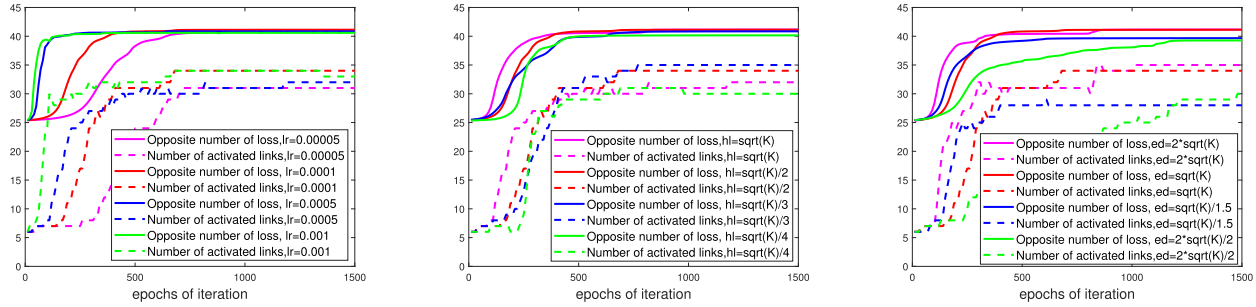

Fig. 13. Relationship between the loss function and the solution objective. (a) Network performance v.s. learning rate. (b) Network performance v.s. hidden layer size. (c) Network performance v.s. dimensions of node embedding.

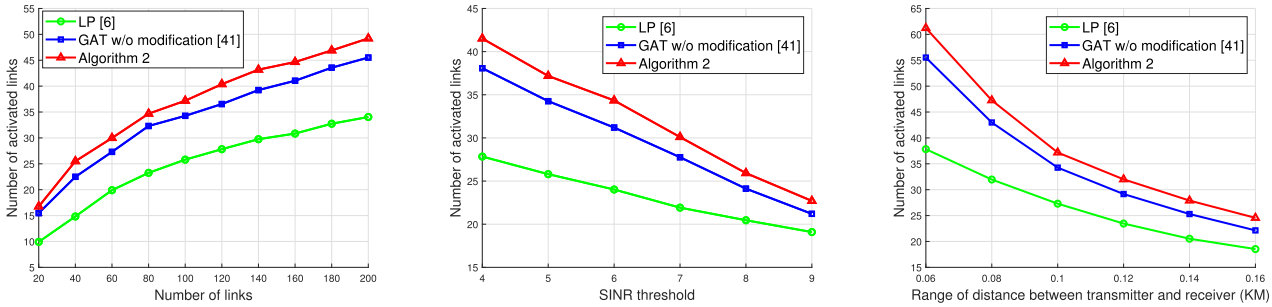

Fig. 14. Simulation results in middle-scale scene. (a) Number of activated links with different number of links. (b) Number of activated links with different interference signal power threshold. ($K = 100$). (c) Number of activated links with different Tx-Rx distance. ($K = 100$).

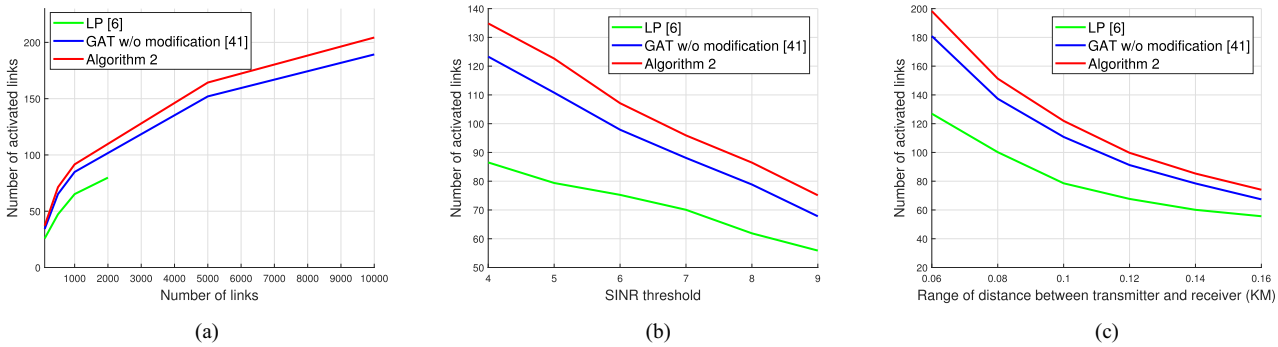

Fig. 15. Simulation results in large-scale scene. (a) Number of activated links with different number of links. (b) Number of activated links with different interference signal power threshold. ($K = 2000$). (c) Number of activated links with different Tx-Rx distance. ($K = 2000$).

this change. This is because when $SINR_t$ is small, GAT can obtain better results by adjusting a large number of weight parameters, while **LP** removes a large number of links due to the relaxation of the integer variables. If $SINR_t$ is increased to a certain limit, the performance of the three algorithms becomes very similar. So, Algorithm 2 is more suitable for the communication scenario with low rate requirement, e.g., the IoT applications.

5) Effect of Tx-Rx Distance on System Performance: Figs. 14(c) and 15(c) demonstrate the effect of the Tx-Rx distance on the number of activated links with different algorithms. As can be observed, Algorithm 2 can activate more links especially for small Tx-Rx distance. The main reason is that neural network can obtain the information of all the links in the scene through iterative update, so as to control the links from a global perspective. Overall, our propose algorithm outperforms the others under any parameter settings, which fully verify its efficiency.

6) Computation Complexity: As shown in Fig. 16, we measure the running time of several algorithms for accumulative interference model at different scene scales. **LP** is iterated in two parts by deleting links and linear programming, where linear programming takes up most of the running time. It has well efficiency performance in small-scale scenarios, but with the increase of the number of links, the time for linear programming operations quickly exceeds the endurance range. In contrast, the

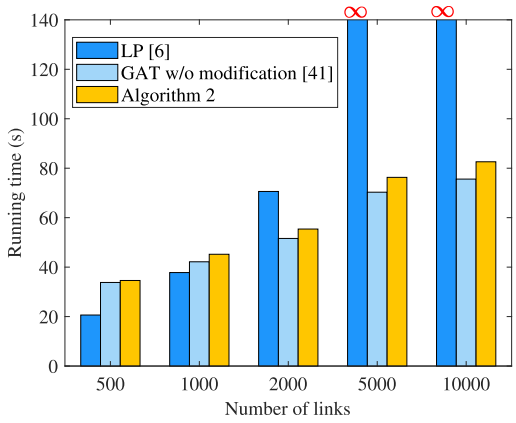

Fig. 16. Running time of accumulative interference model.

TABLE III
SUM TRANSMITTING POWER (WATT)

Number of links	LP	GAT w/o modification	Algorithm 2
50	6.86	4.73	1.46
100	8.51	7.44	2.28
500	11.86	10.69	3.06
1000	13.81	14.78	3.72

natural advantages of machine learning allow **GAT w/o modification** and Algorithm 2 to still make efficient decisions. The extra running time of Algorithm 2 over **GAT w/o modification** is mainly used for the operations described in Section IV-C, which provides considerable performance gains at little time cost. Please note that Remark 2 applies here as well.

7) Energy Saving: In order to discuss the performance of different algorithms in energy saving, we analyze the simulation results of sum of transmitting power. Table III shows that the total power levels of **LP** and **GAT w/o modification** are almost identical, while Algorithm 2 has a very excellent performance in terms of energy consumption, mainly because the operation in Section IV-C improves performance while reducing the transmitted power to the lowest achievable range.

VI. CONCLUSION

In this paper, we have investigated the GNN-based algorithms for solving the joint admission and power control problem in the scenario with massive connections. We have considered two kinds of communication models (i.e., blocking interference model and accumulative interference model) and converted them into graphs to facilitate the use of GNN. For the blocking interference model, we have proposed a GCN-based algorithm with a degree-adaptive loss function. For the accumulative interference model, we have proposed a GAT-based algorithm and adjusted the approximation function of the step function. The optimized schemes have been designed for the output of the GCN and GAT respectively. Finally, extensive simulations have been conducted to verify the performance and computation efficiency of our proposed algorithms. The performance of the GCN-based method can reach 83.8% of the optimal solution within short running time, and the GAT-based method can increase the number of activated links by 43.78% compared to the LP. The advantages of our proposed algorithms in computation efficiency is highlighted with the expansion of scene size.

Noted the proposed approaches in this paper are centralized control schemes. They strike a good balance between performance and computational complexity compared to other algorithms, particularly demonstrating more apparent advantages in massive connections. However, the fact that they must rely on global network state information is a disadvantage, which poses certain challenges in practical applications, especially in dynamically changing scenarios. Therefore, a future research direction is to design the GNN based distributed algorithms. Besides, this paper focuses on the access management problem in a single frequency band. The multi-channel wireless networks are more common, so we can extend it to the multi-channel condition in the future work. Moreover, various applications may have different priorities, so future research should also consider the fairness problem.

REFERENCES

[1] F. Guo, F. R. Yu, H. Zhang, X. Li, H. Ji, and V. C. M. Leung, "Enabling massive IoT toward 6G: A comprehensive survey," *IEEE Internet Things J.*, vol. 8, no. 15, pp. 11891–11915, Aug. 2021.
[2] Q. Qi, X. Chen, C. Zhong, and Z. Zhang, "Integration of energy, computation and communication in 6G cellular Internet of Things," *IEEE Commun. Lett.*, vol. 24, no. 6, pp. 1333–1337, Jun. 2020.
[3] A. H. Sodhro, S. Pirbhulal, Z. Luo, K. Muhammad, and N. Z. Zahid, "Towards 6G architecture for energy-efficient communication in IoT-enabled smart automation systems," *IEEE Internet Things J.*, vol. 8, no. 7, pp. 5141–5148, Apr. 2021.
[4] A. Dogra, R. K. Jha, and S. Jain, "A survey on beyond 5G network with the advent of 6G: Architecture and emerging technologies," *IEEE Access*, vol. 9, pp. 67512–67547, 2021.
[5] C. Wang et al., "On the road to 6G: Visions, requirements, key technologies and testbeds," *IEEE Commun. Surv. Tut.*, vol. 25, no. 2, pp. 905–974, Secondquarter 2023.
[6] Y.-F. Liu, Y.-H. Dai, and Z.-Q. Luo, "Joint power and admission control via linear programming deflation," *IEEE Trans. Signal Process.*, vol. 61, no. 6, pp. 1327–1338, Mar. 2013.
[7] Y.-F. Liu, Y.-H. Dai, and Z.-Q. Luo, "Joint power and admission control via linear programming deflation," in *Proc. IEEE Int. Conf. Acoust., Speech, Signal Process.*, 2012, pp. 2873–2876.
[8] M. Saad and S. Abdallah, "A fast algorithm for power-controlled capacity maximization in wireless networks," in *Proc. IEEE Int. Symp. Signal Process. Inf. Technol.*, 2019, pp. 1–4.
[9] K. B. S. Manosha, S. K. Joshi, M. Codreanu, N. Rajatheva, and M. Latva-Aho, "Admission control algorithms for QoS-Constrained multicell MISO downlink systems," *IEEE Trans. Wireless Commun.*, vol. 17, no. 3, pp. 1982–1999, Mar. 2018.
[10] S. Aboagye, A. Ibrahim, T. M. N. Ngatched, and O. A. Dobre, "Joint user association and power control for area spectral efficiency maximization in HetNets," in *Proc. IEEE 92nd Veh. Technol. Conf.*, Victoria, BC, Canada, 2020, pp. 1–6.
[11] X. Zhai, K. Chen, X. Liu, X. Sun, X. Chang, and B. Chen, "Energy efficiency of access control with rate constraints in cognitive radio networks," *IEEE Access*, vol. 6, pp. 36354–36363, 2018.
[12] W.-S. Lai, T.-H. Chang, and T.-S. Lee, "Joint power and admission control for spectral and energy efficiency maximization in heterogeneous OFDMA networks," *IEEE Trans. Wireless Commun.*, vol. 15, no. 5, pp. 3531–3547, May 2016.
[13] M. Monemi, M. Rasti, and E. Hossain, "Low-complexity SINR feasibility checking and joint power and admission control in prioritized multi-tier cellular networks," *IEEE Trans. Wireless Commun.*, vol. 15, no. 3, pp. 2421–2434, Mar. 2016.
[14] R. Wang, W. Kang, G. Liu, R. Ma, and B. Li, "Admission control and power allocation for NOMA-Based satellite multi-beam network," *IEEE Access*, vol. 8, pp. 33631–33643, 2020.

[15] C.-H. Fang, L.-H. Shen, T.-P. Huang, and K.-T. Feng, "Delay-aware admission control and beam allocation for 5G functional split enhanced millimeter wave wireless Fronthaul networks," *IEEE Trans. Wireless Commun.*, vol. 21, no. 4, pp. 2430–2444, Apr. 2022.
[16] X. Chen, Y. Tang, M. Zhang, and L. Huang, "Ran slice selection mechanism based on satisfaction degree," in *Proc. IEEE Wireless Commun. Netw. Conf. Workshops*, 2020, pp. 1–6.
[17] N. R. Chauhan and R. K. Dwivedi, "Adaptive admission control policy in distributed real time database system," in *Proc. Int. Conf. Syst. Model. Advance. Res. Trends*, 2022, pp. 1057–1062.
[18] M. T. Nguyen and L. B. Le, "Resource allocation, trajectory optimization, and admission control in UAV-Based wireless networks," *IEEE Commun. Lett.*, vol. 3, no. 3, pp. 129–132, Sep. 2021.
[19] S. Kianpisheh and R. H. Glitho, "Joint admission control and resource allocation with parallel VNF processing for time-constrained chains of virtual network functions," *IEEE Access*, vol. 9, pp. 162553–162571, 2021.
[20] X. Zhang, D. Li, and Y. Zhang, "Maximum throughput under admission control with unknown queue-length in wireless sensor networks," *IEEE Sensors J.*, vol. 20, no. 19, pp. 11387–11399, Oct. 2020.
[21] H. Sun et al., "Learning to optimize: Training deep neural networks for interference management," *IEEE Trans.Signal Process.*, vol. 66, no. 20, pp. 5438–5453, Oct. 2018.
[22] M. Eisen, C. Zhang, L. F. O. Chamon, D. D. Lee, and A. Ribeiro, "Learning optimal resource allocations in wireless systems," *IEEE Trans. Signal Process.*, vol. 67, no. 10, pp. 2775–2790, May 2019.
[23] W. Cui, K. Shen, and W. Yu, "Spatial deep learning for wireless scheduling," *IEEE J. Sel. Areas Commun.*, vol. 37, no. 6, pp. 1248–1261, Jun. 2019.
[24] F. Hong, Y. Huang, Y. Xu, D. He, and W. Zhang, "Deep reinforcement learning based mode selection and power allocation scheme for convergent power-efficient network," in *Proc. IEEE Int. Symp. Broadband Multimedia Syst. Broadcast.*, 2022, pp. 1–6.
[25] R. H. Y. Perdana, T.-V. Nguyen, and B. An, "Deep learning-based power allocation in massive MIMO systems with SLNR and SINR criterions," in *Proc. 12th Int. Conf. Ubiquitous Future Netw.*, 2021, pp. 87–92.
[26] U. Demirhan and A. Alkhateeb, "Integrated sensing and communication for 6G: Ten key machine learning roles," *IEEE Commun. Mag.*, vol. 61, no. 5, pp. 113–119, May. 2023.
[27] S. Sarkar and A. Debnath, "Machine learning for 5G and beyond: Applications and future directions," in *Proc. 2nd Int. Conf. Electron. Sustain. Commun. Syst.*, 2021, pp. 1688–1693.
[28] D.-X. Liu, "Reliability analysis and optimization of computer communication network based on machine learning algorithm," in *Proc. Int. Conf. Front. Artif. Intell. Mach. Learn.*, 2022, pp. 42–46.
[29] A. Endes and B. Yuksekkaya, "5G network slicing using machine learning techniques," in *Proc. 30th Signal Process. Commun. Appl. Conf.*, 2022, pp. 1–4.
[30] F. Xia et al., "Graph learning: A survey," *IEEE Trans. Artif. Intell.*, vol. 2, no. 2, pp. 109–127, Apr. 2021.
[31] Z. Wu, S. Pan, F. Chen, G. Long, C. Zhang, and P. S. Yu, "A comprehensive survey on graph neural networks," *IEEE Trans. Neural Netw. Learn. Syst.*, vol. 32, no. 1, pp. 4–24, Jan. 2021.
[32] A. I. Diveev and O. V. Bobr, "NP-Hard task schedules and methods of its decision," in *Proc. IEEE 11th Int. Conf. Appl. Inf. Commun. Technol.*, 2017, pp. 1–5.
[33] L. Schmarje, M. Santarossa, S. M. Schröder, and R. Koch, "A survey on semi-, self- and unsupervised learning in image classification," *IEEE Access*, vol. 9, pp. 82146–82168, 2021.
[34] D. Zhao et al., "A graph convolutional network-based deep reinforcement learning approach for resource allocation in a cognitive radio network," *Sensors*, vol. 20, no. 18, pp. 5216–5220, Sep. 2020.
[35] K. Nakashima, S. Kamiya, K. Ohtsu, K. Yamamoto, T. Nishio, and M. Morikura, "Deep reinforcement learning-based channel allocation for wireless LANs with graph convolutional networks," in *Proc. IEEE 90th Veh. Technol. Conf.*, Honolulu, HI, USA, 2019, pp. 1–5.
[36] Y. Peizhi, C. Salimur, A. T. Fadi, and A. O. lbrhaim, "An energy-efficient topology control algorithm for optimizing the lifetime of wireless ad-hoc IoT networks in 5G and B5G," *Comput. Commun.*, vol. 159, pp. 83–96, Jun. 2020.
[37] Y. Shen, Y. Shi, J. Zhang, and K. B. Letaief, "Graph neural networks for scalable radio resource management: Architecture design and theoretical analysis," *IEEE J. Sel. Areas Commun.*, vol. 39, no. 1, pp. 101–115, Jan. 2021.
[38] Y. Shen, Y. Shi, J. Zhang, and K. B. Letaief, "A graph neural network approach for scalable wireless power control," in *Proc. IEEE Globecom Workshops*, Waikoloa, HI, USA, 2019, pp. 1–6.
[39] N. NaderiAlizadeh, M. Eisen, and A. Ribeiro, "Adaptive wireless power allocation with graph neural networks," in *Proc. IEEE Int. Conf. Acoust., Speech, Signal Process.*, 2022, pp. 5213–5217.
[40] T. N. Kipf and M. Welling, "Semi-supervised classification with graph convolution network," 2016, *arXiv:1609.02907*.
[41] V. Peter, G. Cucurull, A. Casanova, and A. Romero, "Graph attention network," in *Proc. 6th Int. Conf. Learn. Representations*, 2018, pp. 1–12.
[42] L. E. Márquez, A. Osorio, M. Calle, J. C. Velez, A. Serrano, and J. E. Candelo-Becerra, "On the use of LoRaWAN in smart cities: A study with blocking interference," *IEEE Internet Things J.*, vol. 7, no. 4, pp. 2806–2815, Apr. 2020.
[43] J. Zheng, G. Wei, and C. Qi, "Research on blocking interference for digital radio station under UWB EMP," *AIP Adv.*, vol. 11, no. 5, pp. 1–7, May 2021.
[44] M. J. A. Schuetz, J. K. Brubaker, and H. G. Katzgraber, "Combinatorial optimization with physics-inspired graph neural networks," *Nature Mach. Intell.*, vol. 4, no. 4, pp. 367–377, Apr. 2022.

Mengke Yang received the B.E. degree in electronic and information engineering from Chang'an University, Xi'an, China, in 2021. She is currently working toward the M.S. and Ph.D degrees with the School of Electronics and Information, Northwestern Polytechnical University, Xi'an. Her research focuses on wireless communication assisted by graph learning.

Daosen Zhai received the B.E. degree in telecommunication engineering from Shandong University, Weihai, China, in 2012, and the Ph.D. degree in communication and information systems from Xidian University, Xi'an, China, in 2017. He is currently an Associate Professor with the School of Electronics and Information, Northwestern Polytechnical University, Xi'an. His research interests include B5G and 6G key techniques, massive access techniques, air-and-ground integrated network, and convex optimization and graph theory and their applications in wireless communications.

Ruonan Zhang received the B.S. and M.Sc. degrees in electrical and electronics engineering from the Xi'an Jiaotong University, Xi'an, China, in 2000 and 2003, respectively, and the Ph.D. degree in electrical and electronics engineering from the University of Victoria, Victoria, BC, Canada, in 2010. He was an IC Design Engineer with the Motorola Inc. and Freescale Semiconductor Inc., Tianjin, China, from 2003 to 2006. Since 2010, he has been with the Department of Communication Engineering, Northwestern Polytechnical University, Xi'an, where he is currently a Professor. His research interests include wireless channel measurement and modeling, architecture and protocol design of wireless networks, and satellite communications. He was the recipient of the New Century Excellent Talent Grant from the Ministry of Education of China. He was a Local Arrangement Co-Chair for the IEEE/CIC International Conference on Communications in China (ICCC) in 2013, Industry Track and Workshop Chair for the IEEE International Conference on High Performance Switching and Routing (HPSR) in 2019, and as an Associate Editor for *Journal of Communications and Networks*.

Bin Li received the B.S. and Ph.D. degrees in electrical and electronics engineering from Xi'an Jiaotong University, Xi'an, China, in 2006 and 2014, respectively. Since 2014, he has been with the Department of Communication Engineering, Northwestern Polytechnical University, Xi'an, China, and he is currently an Associate Professor. His current research interests include Internet of Things, network coding, MIMO, and wireless channel measurement modeling.

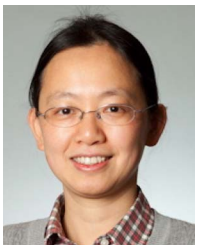

Lin Cai (Fellow, IEEE) has been with the Department of Electrical and Computer Engineering, University of Victoria, Victoria, BC, Canada, since 2005 and is currently a Professor. She is an NSERC E.W.R. Steacie Memorial Fellow, a Canadian Academy of Engineering (CAE) Fellow, an Engineering Institute of Canada (EIC) Fellow, and an IEEE Fellow. In 2020, she was elected as a Member of the Royal Society of Canada's College of New Scholars, Artists and Scientists, and a 2020 "Star in Computer Networking and Communications" by N2Women. Her research interests include communications and networking, with a focus on network protocol and architecture design supporting ubiquitous intelligence. She received the NSERC Discovery Accelerator Supplement (DAS) Grants in 2010 and 2015, respectively. She co-founded and chaired the IEEE Victoria Section Vehicular Technology and Communications Joint Societies Chapter. She has been elected to serve the IEEE Vehicular Technology Society (VTS) Board of Governors, during 2019–2024, and was its VP Mobile Radio from 2023 to 2024. She served as a Board Member of IEEE Women in Engineering from 2022 to 2024, and a Board Member of IEEE Communications Society (ComSoc) from 2024 to 2026. She has held various editorial roles, including Associate Editor-in-Chief for IEEE TRANSACTIONS ON VEHICULAR TECHNOLOGY and membership in the Steering Committee of the IEEE TRANSACTIONS ON MOBILE COMPUTING (TMC), IEEE TRANSACTIONS ON BIG DATA (TBD), and IEEE TRANSACTIONS ON CLOUD COMPUTING (TCC). She has also been an Associate Editor of IEEE/ACM TRANSACTIONS ON NETWORKING, IEEE INTERNET OF THINGS JOURNAL, IEEE TRANSACTIONS ON WIRELESS COMMUNICATIONS, IEEE TRANSACTIONS ON VEHICULAR TECHNOLOGY, IEEE TRANSACTIONS ON COMMUNICATIONS. Lin Cai is a Distinguished Lecturer of the IEEE VTS and IEEE Communications Societies, and a registered professiona engineer in British Columbia, Canada.

F. Richard Yu (Fellow, IEEE) received the Ph.D. degree in electrical engineering from the University of British Columbia, Vancouver, BC, Canada, in 2003. From 2002 to 2006, he was with Ericsson (in Lund, Sweden) and a start-up in California, USA. In 2007, he joined Carleton University, Ottawa, ON, Canada, where he is currently a Professor. His research interests include wireless cyber-physical systems, connected/autonomous vehicles, security, distributed ledger technology, and deep learning. He was the recipient of the IEEE Outstanding Service Award in 2016, IEEE Outstanding Leadership Award in 2013, Carleton Research Achievement Award in 2012, the Ontario Early Researcher Award (formerly Premiers Research Excellence Award) in 2011, Excellent Contribution Award at IEEE/IFIP TrustCom 2010, the Leadership Opportunity Fund Award from Canada Foundation of Innovation in 2009 and the Best Paper Awards at IEEE ICNC 2018, VTC 2017 Spring, ICC 2014, Globecom 2012, IEEE/IFIP TrustCom 2009 and Int'l Conference on Networking 2005. He serves on the editorial boards of several journals, including Co-Editor-in-Chief for Ad Hoc and Sensor Wireless Networks, Lead Series Editor for IEEE TRANSACTIONS ON VEHICULAR TECHNOLOGY, IEEE TRANSACTIONS ON GREEN COMMUNICATIONS AND NETWORKING, and IEEE COMMUNICATIONS SURVEYS AND TUTORIALS. He was the Technical Program Committee (TPC) Co-Chair of numerous conferences. Dr. Yu is a registered Professional Engineer in the province of Ontario, Canada, a Fellow of the Institution of Engineering and Technology (IET). He is a Distinguished Lecturer, the Vice President (Membership), and an elected member of the Board of Governors (BoG) of the IEEE Vehicular Technology Society.